Available online at www.sciencedirect.com

SCIENCE DIRECT

Developmental Biology 277 (2005) 403–416

DEVELOPMENTAL BIOLOGY

www.elsevier.com/locate/ydbio

Basal membrane remodeling during follicle histogenesis in the rat ovary: contribution of proteinases of the MMP and PA families

Séverine Mazaud[a], Romain Guyot[b], Céline J. Guigon[a], Noëlline Coudouel[a], Brigitte Le Magueresse-Battistoni[b], Solange Magre[a,*]

[a]*Laboratoire de Physiologie et Physiopathologie, CNRS-UMR 7079, Université Paris VI, Paris, France*
[b]*INSERM-U329, Hôpital Debrousse, 69322 Lyon Cedex 05, France*

Received for publication 17 April 2004, revised 1 October 2004, accepted 1 October 2004
Available online 27 October 2004

Abstract

In mammalian females, follicular units arise from the fragmentation of ovigerous cords, which spread over the first three postnatal days in the rat. The mechanisms underlying such a process of epithelial remodeling involve a specific balance between basal membrane (BM) deposition and degradation that has as yet not been precisely described. We have investigated the contribution of proteases in BM remodeling by localization of transcripts, protein, or enzymatic activity. In addition, we have analyzed BM deposition at the ultrastructural level and by immunofluorescence detection of BM components. At birth, when fragmentation occurred, epithelial cells displayed an upregulation of membrane type 1-matrix metalloproteinase (MT1-MMP) and urokinase-type plasminogen activator (uPA), as well as laminin α1 mRNAs. Although MMP2 expression was restricted to mesenchymal cells throughout development, in situ zymography showed that gelatinase-MMP2 activity colocalized with BM deposition inside deepening clefts in the areas of ovigerous cord fragmentation. In the days following birth, gelatin and plasminogen-casein zymography showed an increased enzymatic activity of MMP2 and uPA, respectively. In organotypic cultures of 21-day postconception ovaries, serine protease inhibitors like aprotinin could efficiently block follicle histogenesis. In addition, our results show that the well described and great wave of oocyte attrition characteristic of the days following birth closely correlates with BM remodeling. Altogether, our data show that during follicle histogenesis, ovigerous cord fragmentation results from an acute BM component deposition in deepening clefts and that BM homeostasy involves proteinases of the MMP2/MT1-MMP/TIMP3 and plasminogen/uPA families.

Keywords: Epithelial morphogenesis; Basal membrane remodeling; MMP; PA; Oocyte apoptosis

Introduction

In mammalian females, a key step in ovarian differentiation is the formation of follicles, the functional units of the ovary. They appear as unique epithelial structures, composed of a single dictyate quiescent oocyte surrounded by granulosa cells and delimitated by a basal membrane (BM) in close apposition to a mesenchymal tissue destined to differentiate into the thecal layer. The first step of folliculogenesis is the emergence of primordial follicles as a result of the fragmentation of the ovigerous (or ovarian) cords. Ovigerous cords are fetal epithelial structures made up of clusters of pregranulosa cells and germ cells that have entered meiotic prophase (Merchant-Larios and Chimal-Monroy, 1989). In rats, folliculogenesis is initiated during hours following birth and continues for 3–4 days following a typical centrifugal pattern, that is, progressing from the core of the ovary toward the surface epithelium (Rajah et al.,

Abbreviations: dpc, day postconception; dpn, day postnatal; MMP, matrix metalloproteinase; TIMP, tissue inhibitor of MMP; uPA, urokinase-type Plasminogen Activator; tPA, tissue-type Plasminogen Activator; TUNEL, TdT-mediated dUTP-fluorescein Nick End Labeling; AMH, anti-Müllerian hormone; ECM, extracellular matrix; BM, basal membrane.

* Corresponding author. Laboratoire de Physiologie et Physiopathologie, UMR 7079, Université Paris VI, 7 quai Saint-Bernard, 75005 Paris, France. Fax: +33 1 44 27 26 50.
E-mail address: solange.magre@snv.jussieu.fr (S. Magre).

0012-1606/$ - see front matter © 2004 Elsevier Inc. All rights reserved.
doi:10.1016/j.ydbio.2004.10.001

1992). Once differentiated, a subset of follicles localized in the core of the ovary begins to grow (Hirshfield and DeSanti, 1995), and at 3 dpn, the ovary contains primary follicles in the center and primordial follicles at the periphery of the gonad (Rajah et al., 1992).

Although cellular and molecular mechanisms governing follicle assembly are yet a matter of conjecture, it has long been acknowledged that folliculogenesis is strictly dependent on the presence of oocytes. When ovaries are depleted in germ cells due to genetic disorders or following experimental procedures, folliculogenesis fails to take place and ovaries evolve into streak gonads (McLaren, 1991). Normal ovarian morphogenesis implies massive degenerative process of germ cells occurring at several phases of development. One of these degenerative phases takes place concomitantly with initiation of follicle histogenesis (Beaumont and Mandl, 1962; McGee et al., 1998). It has been recently advanced that oocyte apoptosis may play a key role in folliculogenesis (Pepling and Spradling, 2001; Sawyer et al., 2002) in permitting, for example, each surviving oocyte to be associated with an appropriate number of epithelial pregranulosa cells (Sawyer et al., 2002).

At the time of primordial follicle assembly, the overall histoarchitecture of the ovary changes and major modifications in cellular relationships occur not only solely between germ and epithelial cells but also between epithelial and mesenchymal cells. During organogenesis, reciprocal epithelio-mesenchymal interactions are well recognized as critical determinants of morphogenetic processes. They are in part, mediated by the remodeling of the extracellular matrix (ECM) and its epithelial specialization, the BM. Numerous studies reporting on the modifications occurring in either ECM synthesis or degradation via specific proteases have demonstrated, indeed, the key role of ECM component turnover in morphogenetic processes (Stuart et al., 1995; Vu and Werb, 2000). In the ovary, although numerous data exist on the ECM composition during fetal development and in adult period (Pelliniemi and Frojdman, 2001; Rodgers et al., 2000), and on the activity of proteases such as plasminogen activators (PAs), matrix metalloproteinases (MMPs), cathepsins, and ADAM family proteases in the cycling ovary (Curry and Osteen, 2001; Ny et al., 2002; Robker et al., 2000), very little information is available on the exact time of follicular assembly (Rajah and Sundaram, 1994).

In the present work, we have investigated the remodeling of the BM during the process of follicle histogenesis and focused our analysis on the role of MMP and plasmin protease families. To identify cells responsible for synthesis of proteases and ECM components, we studied gene expression by in situ hybridization and completed our study by immunohistochemistry and analysis of protease activity. Cellular relationships were analyzed at the ultrastructural level, and an organ culture approach was performed to test the efficiency of inhibitors of proteasic activities on the initiation of folliculogenesis in vitro.

Materials and methods

Animal handling

Female rats from the Wistar strain (Janvier, 53, Le Genest, France) were housed overnight with males and the following day was considered 0 dpc. Animals were maintained on a 12L:12D schedule. Birth, defined as 0 dpn, generally occurred in the night between 21 and 22 dpc. Ovaries were collected from fetuses at 13, 18, and 20 dpc and from pups at 0, 1, 3, 6, and 12 dpn. Ovaries were either snap frozen for RNA or protein analysis, or processed for in situ studies.

Organotypic cultures

Organ culture experiments were performed on at least four ovaries recovered from 21.5 dpc old females from at least two litters, and six independent experiments were performed. Capsule-dissected ovaries were cultured on steel grids previously coated with 2% agar. Basal culture medium was CMRL 1066 supplemented with penicillin/streptomycin and L-glutamin. Organ culture media were changed after 3 days of culture. The following drugs were added: 20–100 μg/ml α2-macroglobulin (Sigma), 100–200 μM phosphoramidon (Sigma), 100–200 μg/ml aprotinin (Sigma), 100 μM leupeptin (Sigma). After 6 days of culture, ovaries were either processed for in situ hybridization or fixed in Bouin's, embedded in paraffin, 5-μm-thick sectioned, and stained with Tuchmann blue.

Screening of matrix metalloproteinase gene expression pattern by macroarrays

Total mRNA was prepared by the TRI Insta pure method (Eurogentec S.A., Angers, France) from 18, 21 dpc, 0, 1, 3, 10 dpn ovaries and subjected to cDNA macroarray analysis according to manufacturer's instructions (SuperArray, TEBU sa, France). Briefly, 10 μg of total RNA was used as template for [^{32}P] cDNA probe synthesis. The RNA was first annealed with 2 μl of a pathway specific primer mix in a final volume of 20 μl in a thermal cycler at 70°C for 2 min. It was then cooled at 42°C and kept at 42°C for 2 min before the addition of 20 μl of the labeling mix prewarmed to 42°C. The labeling mix contained 5 μl of [α-^{32}P] dCTP (10 μCi/μl, 3000 Ci/mmol, Amersham Pharmacia Biotech), 2 μl of MMLV Superscript reverse transcriptase (50 U/μl; Invitrogen), 1 μl RNase inhibitor (40 U/μl; Roche), 8 μl of 5× labeling buffer (1 mM each of dATP, dTTP, and dGTP, 0.01 mM dCTP and 10 mM $MgCl_2$), and 4 μl of RNase-free H_2O. The reaction mixture was incubated at 42°C for 50 min. The reaction was stopped by the addition of 5 μl of 10× stop solution (100 mM EDTA, pH 8.0). The cDNA probe was denatured by the addition of 5 μl of the denaturation solution 20 min at 68°C, and stopped by the addition of 50 μl of the neutralization solution 10 min at

68°C. The array was prehybridized at 68°C in 5× Sodium chloride/Sodium Citrate (SSC) buffer containing 50% formamide, 5× Denhart's solution, 2% SDS, 10% dextran sulfate, and 100 μg of denatured sheared salmon sperm DNA per milliliter. The cDNA probe was hybridized to the cDNA array overnight at 68°C. The membrane was washed twice with 100 ml of prewarmed 2× SSC, 1% SDS for 20 min at 68°C, and twice with 0.1× SSC, 0.5% SDS for 20 min at 68°C, both with shaking (30–40 rpm/min). The membrane was wrapped in a plastic wrap and exposed to X-ray film with an intensifying screen at −80°C, developed, and scanned by a phosphorimager.

Each membrane was stripped four times. To that purpose, membranes were washed twice with 100 ml of prewarmed 0.1 M NaOH, 0.1% SDS at 65°C, and twice with 100 ml of 0.2 M Tris–HCl, 0.1% SDS at room temperature, both with shaking (30–40 rpm/min). Stripping was verified by exposition to X-ray films and rehybridized with other cDNA probes. Each array is composed of 22 marker genes in duplicate spots, two positive controls, β-actin and GAPDH, and a negative control, bacterial plasmid pUC18.

In situ hybridization

Plasmids containing the PCR-generated cDNAs are described in Table 1. Digoxigenin-labeled riboprobes were generated by in vitro transcription. Ovaries were fixed for 1 h at 4°C in 2% paraformaldehyde, cryoprotected in 12%, 15%, 18% sucrose in PBS, embedded in Tissue-Tek OCT compound (Miles, Inc., Elkhart, IN), and cut into 7-μm-thick sections. In situ hybridization was carried out as previously described (Mazaud et al., 2002).

Terminal deoxynucleotidyl transferase-mediated deoxyuridine 5′-triphosphate-fluorescein nick end labeling (TUNEL)

Detection of apoptotic cells was performed on frozen sections using in situ cell death detection kit, fluorescein (Roche). After PBS washing, sections were fixed in 4% paraformaldehyde in PBS for 30 min at 4°C, rinsed in PBS, and incubated for 1 h at room temperature with the TUNEL reaction mixture containing terminal transferase to label free 3′-hydroxy ends of genomic DNA with fluorescein-labeled deoxy-UTP.

Table 1
Probes used for in situ hybridization

Probes	Accession number	Position	Length
Laminin α1	NM_008480	7101–7453	353
MMP2	NM_031054	662–1393	732
MT1-MMP	NM_031056	278–1139	862
TIMP1	U06179	1–678	679
uPA	NM_008873	425–1078	653
tPA	NM_013151	1940–2401	461
MSY2	AF073954	680–1316	637

Immunofluorescence

Immunofluorescence was performed either directly or on sections previously treated for in situ hybridization or TUNEL labeling using the primary antibodies described in Table 2. After PBS washing, sections were incubated with the primary antibody overnight at 4°C. After PBS washing, slides were incubated with the appropriate secondary either anti-mouse or anti-rabbit Ig biotin-conjugated antibody (diluted 1:200, or 1:500, respectively, Amersham Pharmacia Biotech) for 1 h at room temperature and subsequently with streptavidin-FITC (1:100, Amersham Pharmacia Biotech) or extravidin (1:200, Sigma). TIMP3 immunolabeling was performed on frozen sections of unfixed ovaries following the same procedure. Fluorescence labeling was observed either with a Zeiss epifluorescence microscope or with a Leica TC SP2 confocal microscope.

In situ zymography

Dissected ovaries were cryoprotected in 18% sucrose, embedded in OCT, and cut into 7-μm-thick sections. In situ gelatin zymography was processed as previously described, with some modifications (Duchossoy et al., 2001). Air dried sections were covered with 20 μl substrate reaction mixture (50 mM tris, pH 7.5, 5 mM CaCl2, 0.03% sodium azide containing 50 μg/ml quenched fluorescein-labeled DQ gelatin (EnzCheck, Molecular Probes)) and incubated 12–18 h at room temperature in a humid chamber. After a brief rinse in PBS, sections were covered with mounting medium containing *p*-phenylen-diamin and observed with fluorescent microscopy (Zeiss). A fluorescent signal appeared only after enzymatic cleavage of DQ gelatin, thus revealing local net gelatinase activity on the sections. Control sections incubated with DQ gelatin in substrate buffer containing 10 mM EDTA showed extremely low levels and nonspecific fluorescence. To localize zones subjected to BM deposition in combination with gelatinolytic activity, primary antibody against laminin (Table 2) was directly added to the in situ zymography reaction buffer and incubated overnight at room temperature. After several washes in PBS, the sections were incubated for 2 h at room temperature with Texas red-labeled secondary antibody diluted in PBS–0.05% BSA (1:100, Amersham Pharmacia Biotech). No immunoreactivity was obtained in control sections processed for in situ zymography and incubated with the secondary antibody alone.

Protein extraction and zymography

Ovarian extracts were prepared using phosphate buffer saline (PBS) containing 1% NP-40 and 5 mM EDTA. Protein levels were measured by BCA protein assay (Pierce, Interchim-France).

For gelatin zymography, proteins (25 μg) were electrophoresed at 4°C on 10% polyacrylamide gels containing

Table 2
Antibodies used for immunofluorescence analysis

Antigen	Nature	Dilution	
Fibronectin	Rb polyclonal Ab	1/100	Sigma
Laminin	Rb polyclonal Ab	1/400	Sigma
Collagen IV	Rb polyclonal Ab	1/50	AbCys
Cytokeratin 8 (LE-41)	Ms monoclonal Ab	1/5	Dr. Lane
TIMP3	Rb polyclonal Ab	1/200	Chemicon

1 mg/ml gelatin (Sigma) in the absence of any reducing agent (Guyot et al., 2003; Longin et al., 2001). Following electrophoresis, SDS was removed from the gel by exchange in Triton X-100 (two washes of 30 min at room temperature in 2.5% Triton X-100 followed by two washes of 20 min in distilled water). The gel was subsequently incubated at 37°C for 48 h in 100 mM Tris-base, pH 7.6, containing 15 mM $CaCl_2$. In these conditions, gelatinases present in the samples renatured and autoactivated. White zones of lysis indicating gelatin degrading activity were revealed by staining with Coomassie Brillant blue R-250.

For plasminogen zymography, 20–40 μg were electrophoresed at 4°C on 8% polyacrylamide gels in the absence of any reducing agent. Following electrophoresis, SDS was removed from the gel by exchange in Triton X-100 (two washes of 30 min at room temperature in 2.5% Triton X-100 followed by three washes of 30 min in distilled water). The gel was subsequently placed on a casein-agar-plasminogen underlay essentially as described (Odet et al., 2004; Tolli et al., 1995). Plasminogen degrading activity was visualized after incubation at 37°C for 24–48 h, and gels were scanned.

Electron microscopy

A total of 14 ovaries were recovered at 18, 21 dpc, 0, 1 dpn from Wistar females. Ovaries were dissected from the ovarian capsule, fixed for 24 h at 4°C in 2% paraformaldehyde, 0.5% glutaraldehyde in 0.1 M cacodylate buffer (pH 7.2). After rinsing in the same buffer, tissues were postfixed for 2 h at room temperature in 2% osmium tetroxide (OsO_4) in 0.1 M cacodylate buffer (pH 7.2). Tissues were then dehydrated through a graded series of ethanol and embedded in Epoxy Embedding Resin (Fluka, Sigma). One-micron sections were stained with methylen blue and safranin red, selected blocks were thin sectioned, and grids were stained with uranyl acetate and lead citrate. Electron micrographs were taken on a Zeiss EM906 electron microscope.

Results

Throughout this study, the aspect of the ovary at the exact time of the fragmentation of ovigerous cords at 0 and 1 dpn was compared with that of fetal ovaries (at 18 dpc) and that of ovaries in which folliculogenesis was clearly established (from 6 dpn onwards).

Cellular relationships and basal membrane deposition during follicle histogenesis

In 18 dpc ovaries, ovigerous cords appeared as large clusters of germ cells and epithelial pregranulosa cells (Fig. 1A) delimited by a continuous BM (Fig. 1B, arrows) positive for collagen IV (Fig. 1C). The nuclei of epithelial cells, characterized by an irregular cuboidal shape (Figs. 1A and B), were mainly located at the periphery of the ovigerous cords (Fig. 1A, arrowheads). Outside ovigerous cords, mesenchymal tissue positively stained for fibronectin (Fig. 1D) was composed of spindle-shaped cells, with scarce cytoplasm, orientated with their long axis parallel to the surface of the ovigerous cords (Figs. 1A and B).

From the day of birth onwards, when follicular units emerged from regressing ovigerous cords, epithelial cells underwent a conformational change and became flattened around each oocyte (Fig. 1E). Mesenchymal cells first maintained their orientation parallel to the surface of fragmenting ovigerous cord (Fig. 1E, dotted boxed area) and later on migrated to surround follicular units already delineated by a continuous BM (white boxed areas in Fig. 1E). The incipiency of follicle histogenesis was recognized, at the ultrastructural level, by the progressive formation of narrow clefts between epithelial cells of the ovigerous cords (Fig. 1F). It was noticeable that, at that time, a continuous BM was present within the clefts without intrusion of mesenchymal cells (Fig. 1F). Neither discontinuities in BM

Fig. 1. Differentiation of epithelio-mesenchyme interface and BM deposition during follicle histogenesis. Electron micrographs show the interface between the epithelial and the mesenchymal compartments in 18 dpc ovaries (A–B). Mesenchymal cells are densely aggregated alongside the ovigerous cords. The ovigerous cord basal membrane is localized with arrows (B). Cuboid epithelial cells are packed together at the periphery of the ovigerous cord (arrowheads). Boxed area in A corresponds to B. Immunodetection of collagen IV (C) and fibronectin (D) in 18.5 dpc ovaries shows fibronectin-negative ovigerous cords delineated by a continuous collagen IV-positive BM. Electron micrographs of a 1-dpn ovary show a remodeling area in which follicular units are differentiating (E–F). Regions boxed in E indicate different points of cleavage of the ovigerous cord. Black boxed area f corresponds to the higher magnification F. Before fragmentation occurs, mesenchymal cells maintain their orientation parallel to the surface of the ovigerous cord (white dotted area, E). During fragmentation, BM appears on edges of both separating epithelial units (arrows in F). There is no cytoplasmic process from the neighboring mesenchymal cell in this forming cleft. Progressively mesenchymal cytoplasmic processes become visible between neoformed follicular units (white boxed areas in C). Immunodetection of collagen IV in 0-dpn ovaries (G and H) shows the deposition of BM component inside the ovigerous cords (arrows in H). H is a higher magnification of the region boxed in G. Double labeling of fibronectin by immunofluorescence (I) and laminin α1 subunit mRNAs by in situ hybridization (J) shows that laminin α1 is upregulated in remodeling areas (arrows) while it retained basal levels in still-resting peripheral ovigerous cords (arrowheads). mes., mesenchymal compartment; ov. c., ovigerous cord; mes. c., mesenchymal cell; epi. c., epithelial cell; oo., oocyte. Original magnifications were (A) ×1000, (B) ×2784; (E) ×2090; (F) ×11500. Scale bars: 100 μm in C, D, G, I, and J, and 50 μm in H.

nor contacts between epithelial and mesenchymal cells were observed. At the molecular level, the beginning of folliculogenesis was illustrated by the deposition of BM components, collagen IV (Figs. 1G and H), fibronectin (Fig. 1I), and laminin (not shown) within the ovigerous cords. Interestingly, at the exact time of ovigerous cord fragmentation, we observed an upregulation of the expression of gene coding laminin α1 chain in epithelial cells. The in situ hybridization signal for laminin α1 chain, weak in ovigerous cords, increased noticeably when follicles were forming (Fig. 1J), and was maintained at a high level in granulosa cells of growing follicles (not shown).

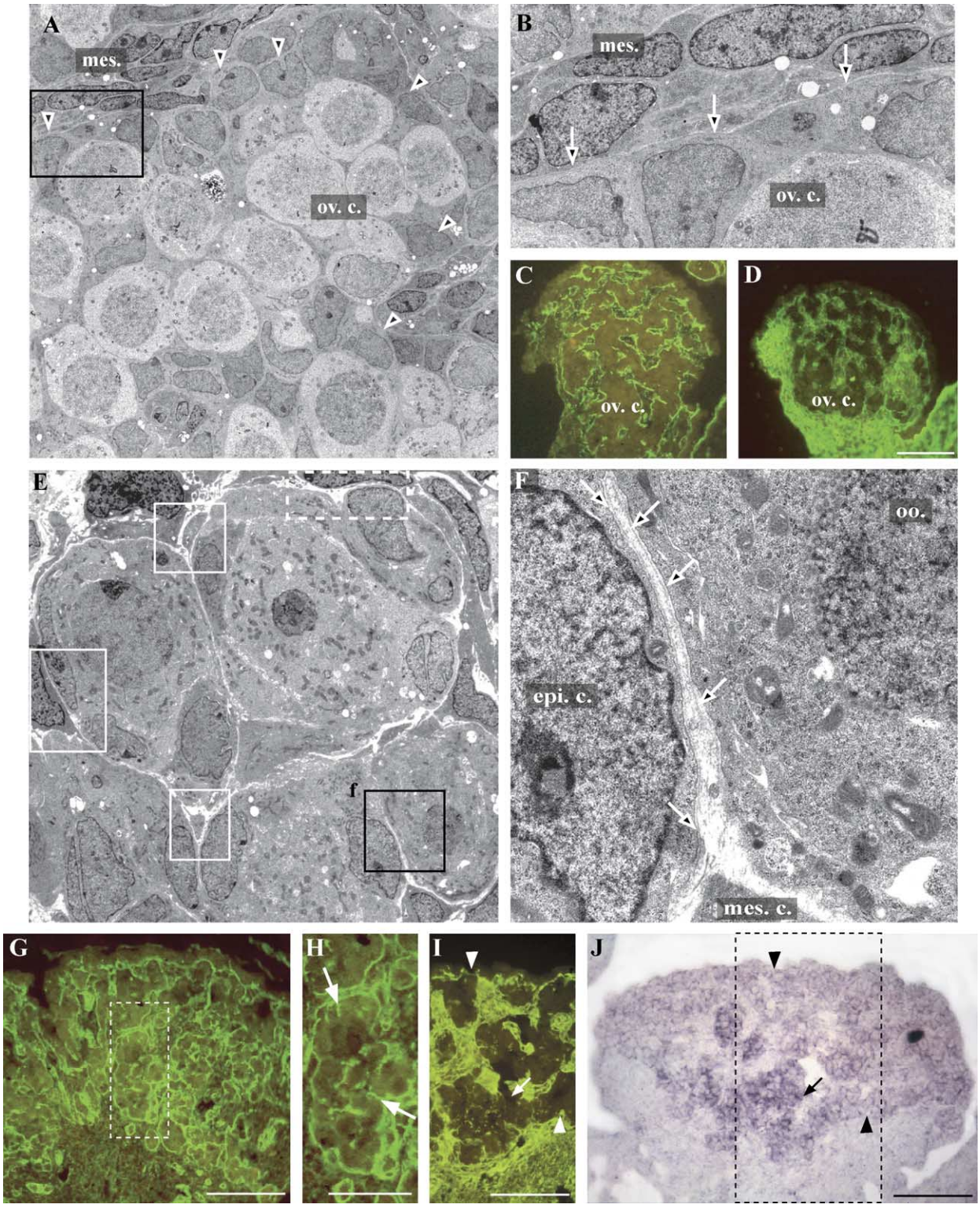

Relationships between oocyte apoptosis and follicle histogenesis

To assess relationships existing between oocyte attrition and BM remodeling in postnatal ovaries, we undertook a comparative study of the distribution of apoptotic (TUNEL-positive) oocytes and the deposition of fibronectin in BM using a confocal approach (Figs. 2A–C). The wave of oocyte apoptosis and the progression of follicle histogenesis followed the same centrifugal pattern: at 0 dpn, apoptotic oocytes were located essentially in the core of the ovary (Figs. 2A and B) and at 1 dpn, principally in the peripheral region (Fig. 2C). Ultrastructural analysis of 1-dpn ovaries (Figs. 2D–G) confirmed that apoptotic oocytes were essentially located in regions where fragmentation had just initiated. In these areas, epithelial cells were not completely flattened around oocytes. Nevertheless, a BM was progressively insinuating between cells in the clefts deepening inside the ovigerous cords (Figs. 2E and F). No BM discontinuity could be observed at the vicinity of atretic oocytes (data not shown). In the central regions of the remodeling ovigerous cords, epithelial cells appeared to separate from one another, revealing extracellular spaces (Fig. 2G). Altogether, these data show the existence of a close relationship between oocyte attrition and ovigerous cord remodeling.

Synthesis and activity of proteases

The plasmin system is composed of two major proteases: urokinase-type (uPA) and tissue-type PA (tPA), both responsible for the activation of the plasminogen into the potent plasmin protease. Transcripts encoding uPA were found in epithelial cells of the fetal ovigerous cords (Figs. 3A and B). At birth, a more intense signal was observed both in epithelial cells and oocytes in areas of fragmentation (Figs. 3C and D, arrows). These levels were maintained in granulosa cells and oocytes of follicles (Fig. 3E). Transcripts encoding tPA were found only in oocytes of growing follicles and not in those of primordial follicles (at 6 dpn, Fig. 3F). To determine the relative importance of the enzymatic activity of the proteases of the plasminogen activator system, we used plasminogen-casein zymography to compare fetal and postnatal ovaries at several ages (Fig. 3G). tPA activity was hardly detectable and uPA activity displayed a biphasic increase: after birth and from 6 dpn onward.

To identify the components of the MMP and tissue-specific inhibitors of MMP (TIMPs) system expressed in the course of follicle histogenesis, we used cDNA macroarrays (Fig. 4A). Among the 18 MMP members and the four TIMPs arrayed, MMP2, membrane type 1 (MT1)-MMP, and TIMP3 were the major matrix metalloproteinases and inhibitor expressed in fetal gonads (at 13.5, 18.5, and 20 dpc, Fig. 4A and data not shown) as well as in neonatal ovaries (at 0, 3, and 10 dpn, Fig. 4A and data not shown). No significant change in their respective level of expression could be detected, with the exception of a relative increase of TIMP3 levels after birth. MMP2, MT1-MMP, and TIMP3 expression was further examined by ISH. Transcripts encoding MMP2 were expressed in mesenchymal cells surrounding epithelial structures, that is, ovigerous cords and follicles (Figs. 4B–E). No variation in the intensity of the signal was found in the ovary at the moment of ovigerous cord fragmentation (Fig. 4C). Transcripts encoding MT1-MMP were present in epithelial cells and in the neighboring mesenchymal cells at all stages (Figs. 4F–N). However, the intensity of the signal was stronger within the areas of fragmentation at 0 dpn (Figs. 4K and L). TIMP3 immunolocalized in the mesenchymal compartment (Figs. 4O–Q).

Since MMPs are synthesized as inactive zymogens, completion of the study required an evaluation of proteasic activity by in situ zymography and SDS-PAGE gelatin zymography (Fig. 5). With the first technique, gelatinolytic activity is monitored via the breakdown of fluorescein-coupled gelatin, yielding highly fluorescent peptides, whereas fluorescence is quenched in undigested gelatin (Figs. 5 A–J). Local increases of fluorescence intensity, thus, reflect a net gelatinase activity at the cellular level. Immunodetection of laminin on the same sections revealed that MMP activity was essentially localized in the mesenchyme. As fragmentation started in central parts of 0-dpn ovaries, gelatinase activity co-localized with thin deposits of laminin inside the fragmenting ovigerous cords (Figs. 5C, D, and H). At 6 dpn, gelatinase activity was present in the mesenchymal tissue and co-localized with the BM surrounding growing follicles. To verify that the gelatinolytic activity actually resulted from MMP activity, we used EDTA, an inhibitor of calcium- and zinc-dependent MMP that has no effect on the other classes of proteases. EDTA (10 mM) abolished the fluorescent pattern found in ovarian sections (Fig. 5J). These data suggested that gelatinase activity and laminin deposition were occurring in the same restricted areas. Since the gelatinolytic activity could be attributed to several MMPs, that is, MMP2, 9, and 3, we used SDS-PAGE gelatin zymography to determine which protease was responsible for the MMP activity in fetal and postnatal ovaries (Fig. 5K). Consistent with the macroarray data, we observed a major group of lytic bands migrating at sizes corresponding to the pro (72 kDa), intermediate (66 kDa), and active (62 kDa) forms of MMP2. The most relevant data were that in fetal and postnatal ovaries from 12 dpn on, the inactive intermediate pro-MMP2 form was the most abundant, whereas the major form observed in 1, 3, and 6 dpn ovaries was the active and mature form of MMP2 (Fig. 5K).

In vitro perturbation of follicular histogenesis

To dissect further the part of the degradation of BM components in follicle histogenesis, fetal ovaries were

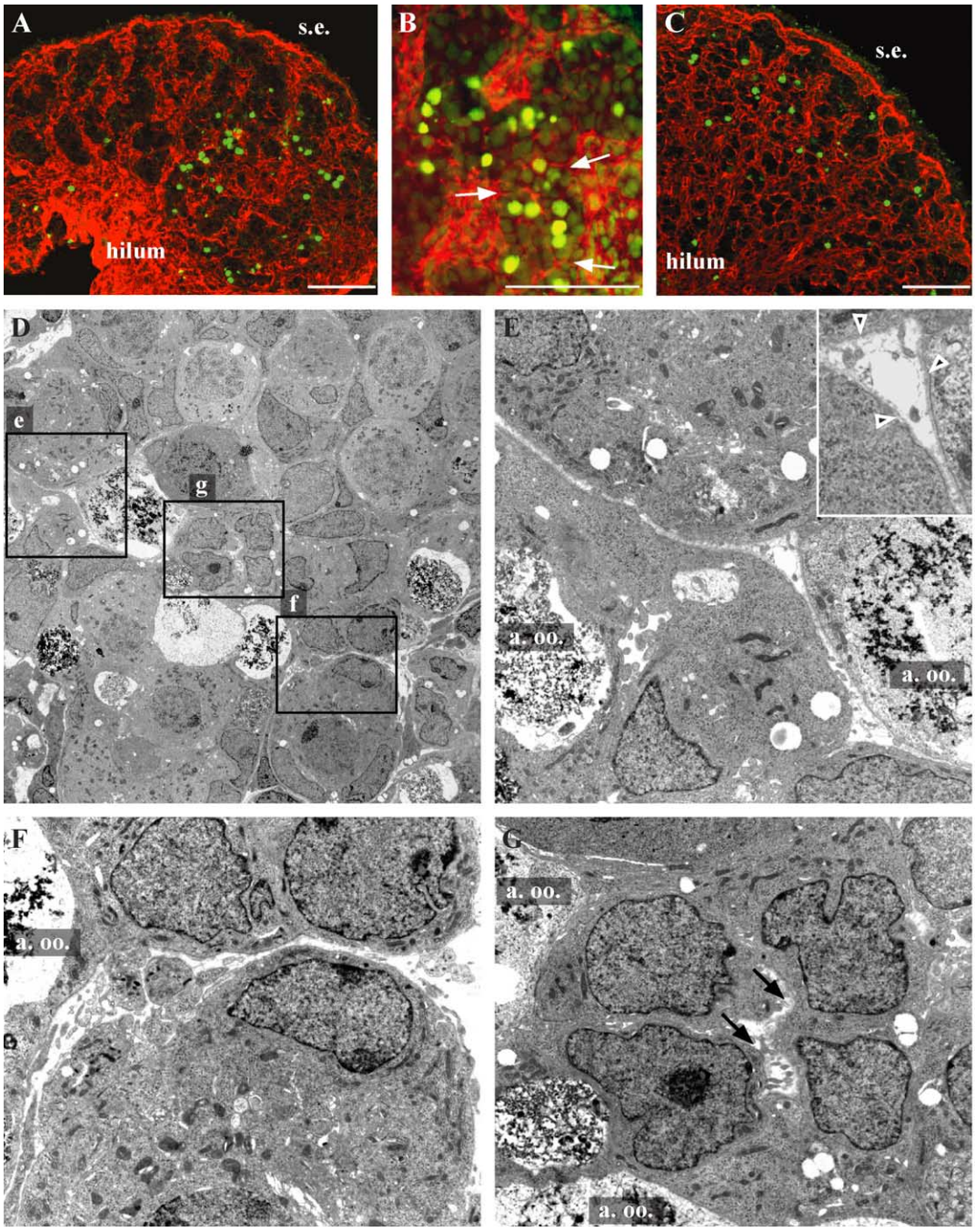

Fig. 2. Relationships between basal membrane deposition and oocyte apoptosis. (A–C) Confocal analysis of basal membrane deposition (fibronectin immunofluorescence, red) and apoptosis (TUNEL technique, green) at 0 (A and B) and 1 dpn (C) shows the spatial correlation between ovigerous cord fragmentation and oocyte apoptosis. At 0 dpn, apoptotic oocytes are located in areas where fibronectin deposits are found inside cords in the core of the ovary, close to the hilum (A and B, arrows). At 1 dpn, apoptotic oocytes are present at the border between neo-formed follicular units and unfragmented ovigerous cords beneath the surface epithelium. (D–G) Ultrastructural analysis of a 1-dpn ovary shows a characteristic aspect of a fragmenting ovigerous cord containing numerous apoptotic oocytes (D, large view). Boxed areas e, f, and g in D correspond to E, F, and G, respectively. Inset in E is a higher magnification of BM deposition pinpointed by arrowheads. Apoptotic oocytes (a. oo.) are essentially located at the endpoint of deepening clefts (E and F). Inside the ovigerous cord, extracellular spaces become visible between somatic cells that begin dissociating (arrows, G). s.e., surface epithelium; a. oo., apoptotic oocytes. Scale bar in A–C = 100 μM. Original magnifications were (D) ×1000, (E–G) ×3597, and (inset in E) ×7200.

dissected at 21.5 dpc before the onset of follicle assembly and cultured for 4 or 6 days in a synthetic medium in the absence or presence of inhibitors of protease activity (Table 3). Oocyte presence was checked by localization of *Msy2* transcripts, which are expressed in diploten oocytes (Gu et al., 1998), and follicle histogenesis was followed by classical histological analysis and by the immunodetection of collagen IV (Fig. 6) and laminin (data not shown) in BM.

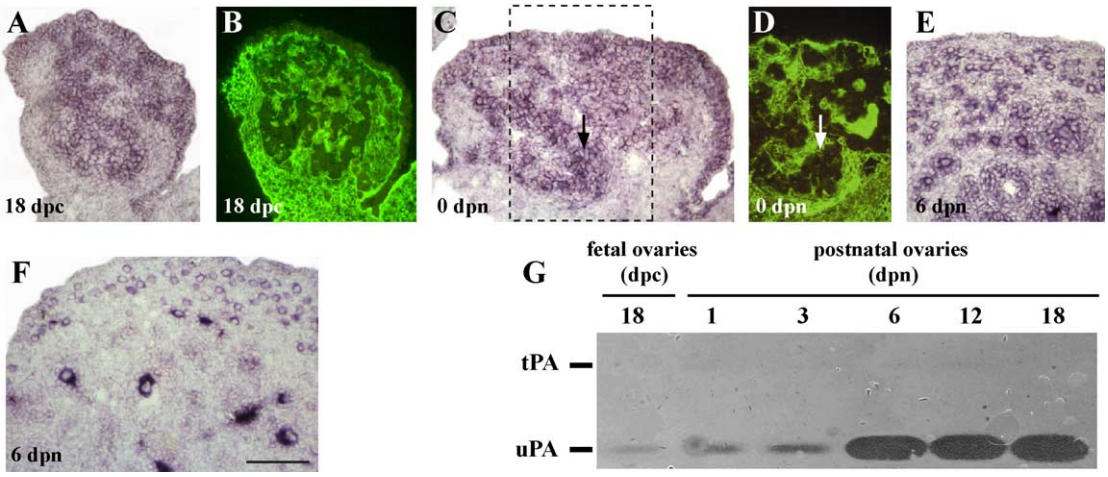

Fig. 3. Expression pattern and enzymatic activity of proteases of the plasmin system. (A–F) Expression patterns of uPA (A, C, and E) and tPA (F) were analyzed by in situ hybridization on 18 dpc (A), 0 (C) and 6 dpn (E and F) ovarian sections. B corresponds to a serial section of A immunostained for fibronectin. D corresponds to the region boxed on C after immunolabeling of fibronectin. Basal levels of uPA transcripts are found in the epithelial compartment of fetal ovaries negative for fibronectin (A and B). At 0 dpn, remodeling ovigerous cords present a more intense signal for uPA (arrow) than that found in still resting ovigerous cords located at the periphery of the ovary (C and D). Transcripts for uPA are later found in granulosa cells and oocytes (E). Transcripts coding tPA are present in oocytes with an increasing signal correlated with follicular growth (F). Scale bar: 100 μm. (G) Plasminogen-casein zymography from ovaries collected before or after birth on the day specified reveals a predominant activity of uPA at all ages. uPA activity increases moderately after birth and markedly from 6 dpn on. Migrations of plasminogen activators are indicated on the left of the panel. This representative casein zymogram was photographed after 22 h of incubation at 37°C.

Whatever the treatment, oocytes were numerous (Figs. 6A and B) and had reached diplotene stage (Figs. 6C and D). In control culture medium, follicle histogenesis was initiated, and primordial and primary follicles were present in the central part of the ovary (Figs. 6A and E). We detected them in all sections passing through the hilum of the ovary (Table 3). At the periphery of the ovary, however, fetal cord organization was maintained (Fig. 6E).

In the presence of potent inhibitors of the plasmin system, either aprotinin or to a lesser extent leupeptin, follicles did not differentiate (Table 3). Thin cords delineated by a collagen IV- and laminin-positive BM were observed. They contained oocytes and epithelial cells (Figs. 6B and F) with a ratio similar to that of follicles (Figs. 6A and E). In the presence of low doses of α_2-macroglobulin (10–20 μM), as well as phosphoramidon, a partial or inconstant inhibition of the initiation of follicle histogenesis occurred, that is, follicles were occasionally observed in the core of the ovary (Table 3). We, thus, obtained a blockage of the fragmentation of the ovigerous cords by inhibiting protease activity, with a more potent effect when inhibiting the plasmin system.

Discussion

In this study undertaken to assess molecular and cellular mechanisms involved in the BM remodeling at the onset of folliculogenesis, our ISH results revealed that the major modifications in the expression of genes encoding for proteases or ECM components occurred in epithelial pregranulosa cells. These modifications were initiated concomitantly with the first histoarchitectural changes of the ovary, that is, when epithelial cells began to encircle individual oocytes and became surrounded by a continuous BM. It is noticeable that changes in the organization of mesenchymal tissue occurred somewhat later, when mesenchymal cells insinuated between the follicular units already delineated by a continuous BM.

Follicle histogenesis results from the fragmentation of ovigerous cords, which is materialized by the deposition of fibronectin, laminin, and collagen IV in deepening clefts that separate forming follicular units. Previous detailed studies on the composition of ECM during gonadogenesis have revealed differences and transitions in the expression pattern of the different isoforms of BM components according to the developmental stage and the state of differentiation (Pelliniemi and Frojdman, 2001). For example, collagen IV α1 and α2 chains that are present in the BM of the fetal rat ovary become restricted to the theca in postnatal ovaries, whereas follicular BM is stained for α3 and α5 chains (Frojdman et al., 1998; Pelliniemi and Frojdman, 2001). Previous studies have shown that, at the time of follicle histogenesis, collagen IV (α1) chain transcripts are acutely synthesized by both epithelial cells and mesenchymal cells surrounding ovigerous cords (Rajah and Sundaram, 1994). Interestingly, our results reveal that the epithelial expression of laminin α1 was upregulated in the areas of tissue remodeling concomitantly with the onset of folliculogenesis. Thereafter, levels remained high within granulosa cells. Generally, maturation of epithelial sheets, with only a few exceptions, is accompanied by a gradual loss of laminin α1 and an increase in laminin α5 chain (Falk et al., 1999). The ovary is atypical in that laminin α5 chain,

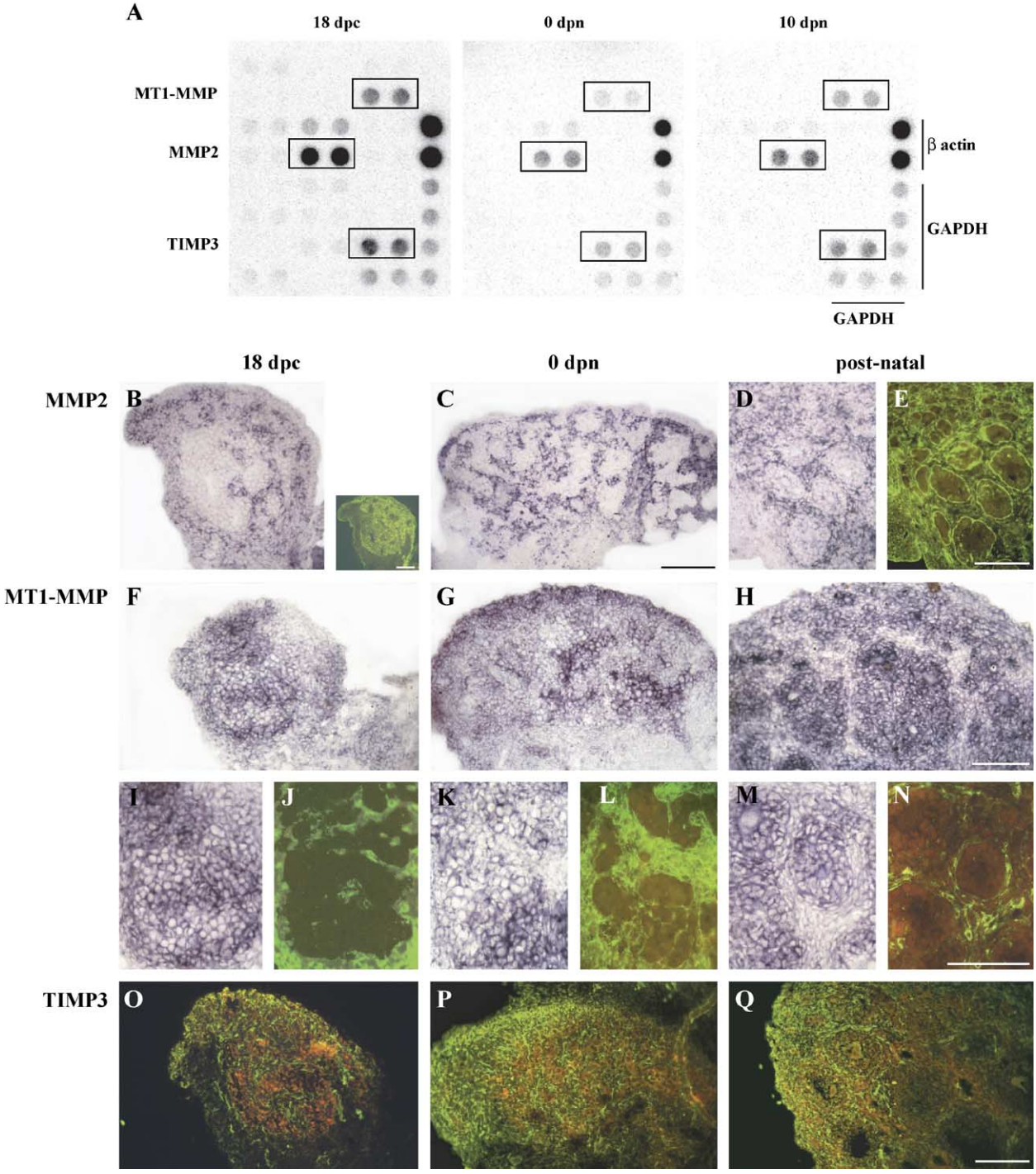

Fig. 4. Expression pattern of the components of the MMP system. (A) Proteases expressed in ovaries around the time of follicular histogenesis were screened by macroarrays. Representative pictures of macroarrays hybridized with radiolabeled cDNAs from 18 dpc, 0 and 10 dpn ovaries. Each gene is present in duplicate. The positive controls β actin and glutaraldehyde-3-phosphate dehydrogenase (GAPDH) are shown at the right and bottom. The negative control bacterial plasmid pUC18 is not expressed in any of these arrays. Three genes are expressed at high levels: MMP2, MT1-MMP, and TIMP3. (B–E) In situ hybridization for MMP2 reveals a mesenchymal expression pattern at 18 dpc (B), 0 (C) and 6 dpn (D). Inset in B corresponds to a serial section immunostained for cytokeratin 8, present in epithelial cells of ovigerous cords. Fibronection immunodetection on the same section as D illustrates follicular organization (E). (F–N) In situ hybridization for MT1-MMP at 18 dpc (F and I), 0 (G and K) and 6 dpn (H and M) and double labeling for fibronectin (J, L, and N) on the same sections as I, K, and M, respectively, were realized. MT1-MMP transcripts were found in epithelial cells of the ovigerous cords and in the immediately surrounding mesenchymal cells at 18 dpc (F and I–J). At 0 dpn, they are found in epithelial cells of the ovarian surface and are upregulated in epithelial cells and oocytes of the fragmenting ovigerous cords (G and K–L). At 6 dpn, MT1-MMP transcripts are present in oocytes, granulosa, and mesenchymal cells surrounding follicles (H and M–N). (O–Q) Immunodetection of TIMP3 shows the protein in strands of mesenchymal cells at 18 dpc (O), 0 (P), and 12 dpn (Q). Mesenchymal cells close to the ovarian surface also express TIMP3 after birth (P and Q). Scale bar: 100 μm.

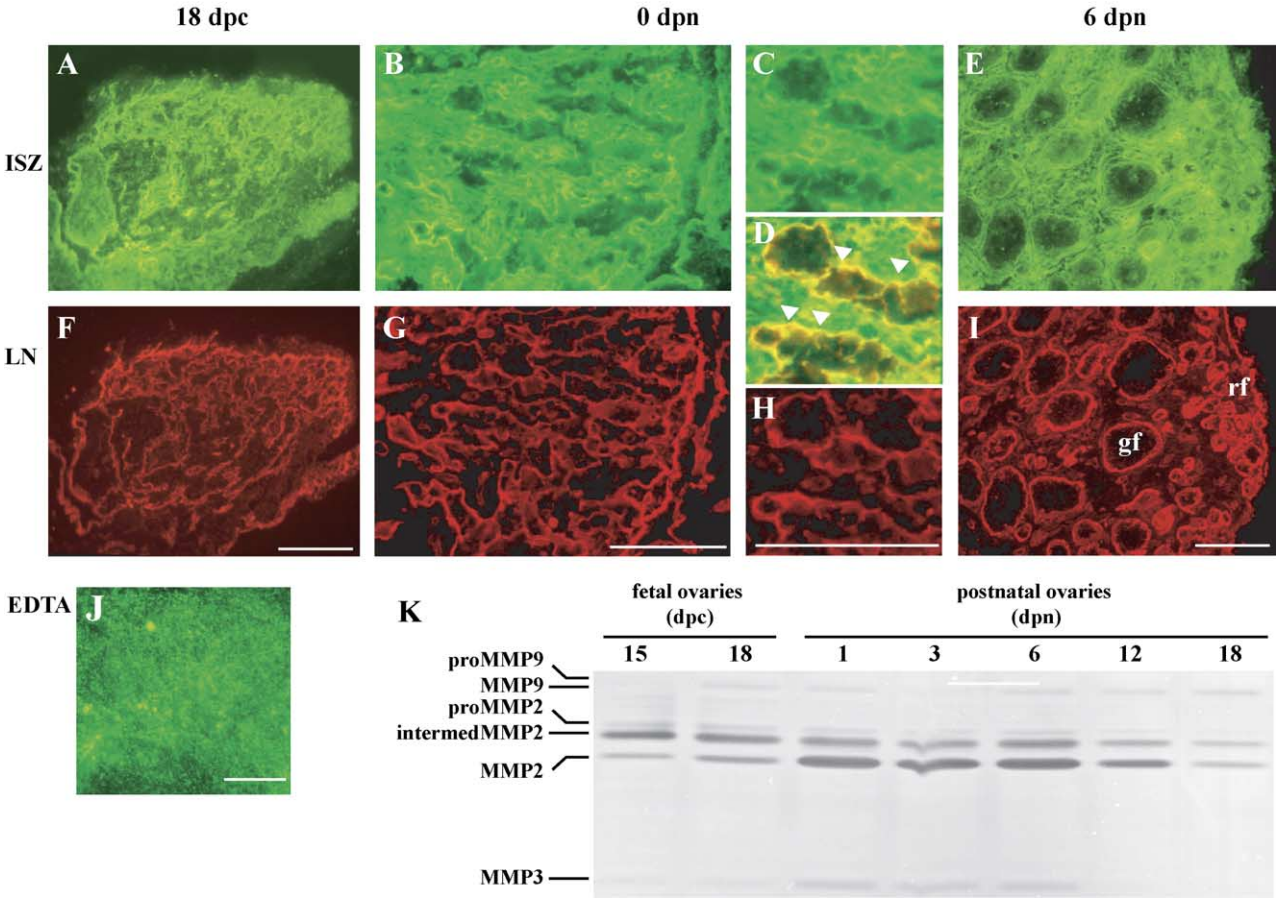

Fig. 5. Proteasic activity of collagenases. (A–J) Spatial correlation between gelatinase activity (A, B, C, and E) and laminin immunolabeling (F, G, H, and I) in 18 dpc (A and F), 0 (B–D and G–H) and 6 dpn ovaries (E and I). C and H are higher magnifications of B and G, respectively, and D is the merged image of C and H. In situ gelatin zymography (ISZ) on fresh frozen sections reveals a strong gelatinase activity in the mesenchyme at all ages. Laminin (LN) immunofluorescence on the same sections stains BM. At 0 dpn, gelatinase activity and laminin immunolabeling are co-detected in thin BM layers insinuating inside the ovigerous cords (arrowheads in D). The gelatinase activity is completely abolished in the presence of 10 mM EDTA (EDTA) (J). gf, growing follicles; rf, resting folicles. Scale bars: 100 μm. (K) Gelatin zymography from ovaries collected before or after birth on the day specified reveals the inactive pro and intermediate forms and the active mature MMP2. The predominant activity is that of the intermediate form of MMP2 before birth, that of the active MMP2 in the days following birth, and the activity becomes equilibrated between the intermediate and the mature forms from 12 dpn on. This representative zymogram is shown as a negative image. Migrations of MMP9 and MMP2 pro, intermediate, and mature collagenases and of MMP3 are indicated on the left of the panel.

present in ovarian fetal BM and in BM of primordial follicles, disappears concomitantly with the maturation of follicles as they begin to secrete anti-Müllerian hormone (AMH) (Frojdman et al., 1999). Moreover, laminin α1 is present in fetal as well as in adult ovaries (this study and in the mouse, Frojdman et al., 1995). The localized upregulation of gene expression we observe at 0 dpn in epithelial cells of the remodeling areas may illustrate the acute contribution of laminin α1 to the synthesis of the BM of creating follicular units.

In addition to synthesis and assembly of ECM molecules, remodeling of BM requires activity of specific proteases that

Table 3
Effect of inhibitors on in vitro fragmentation of the ovigerous cords

	Nature	Concentration	n †	Ovigerous cords fragmentation
1066	Control		17	++
α2-Macroglobulin	Most endoproteinases inhibitor	20–100 μM	11	+/−
Phosphoramidon	Metalloendopeptidases inhibitor	100–200 μM	17	+/−
Aprotinin	Ser proteases inhibitor	100–200 μg/μl	16	−
Leupeptin	Ser and Cys proteinases inhibitor	100 μM	10	+/−

n †: total number of ovaries tested. Experiments were repeated on two to seven separate litters.
Ovigerous cord fragmentation was estimated on a scale from: ++, follicles were present in the core of the ovary in sections passing through the hilum; +/−, follicles were present occasionally, not in all sections; −, no follicles were formed.

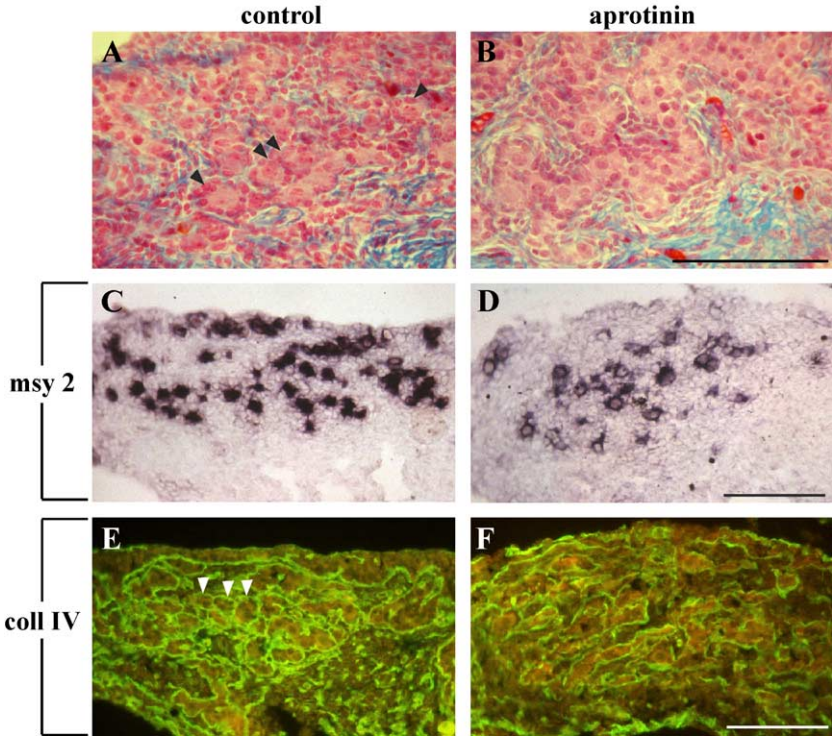

Fig. 6. In vitro perturbation of follicular histogenesis. Fetal ovaries (21.5 dpc) cultured for 4–6 days in control medium (A, C, and E) or in the presence of aprotinin (200 μg/ml) (B, D, and F) were processed for classical histology (A and B) for detection of Msy2 transcripts in germ cells by in situ hybridization (C and D) and for immunolocalization of collagen IV (E and F). Note the forming follicular units in the center of ovaries cultured in control medium (arrowheads) compared to the thin epithelial cords in aprotinin-treated ovaries. Scale bar: 100 μm.

insure the breakdown of its components and, thus, control its composition and turnover. In the rodent ovary, the reciprocal expression of uPA and tPA during follicle development and ovulation has suggested that proteases of the plasminogen activator family have different functions in the ovary (Hagglund et al., 1996; Li et al., 1997). In the rat, uPA is important for BM turnover that accompanies follicle growth specifically in the smallest follicles, and tPA is involved in follicular wall remodeling before ovulation (Li et al., 1997). Our observations have demonstrated that uPA displays a spatial and temporal upregulation at the transcript and enzymatic activity levels at the onset of follicle histogenesis. This suggests that uPA, in addition to its role in the BM remodeling necessary for follicle maturation (Li et al., 1997), could also possibly be implicated in the process of follicular histogenesis. Regarding tPA expression, we detected neither transcripts nor enzymatic activity at the time of initial folliculogenesis. In agreement with previous data (Li et al., 1997), transcripts were detected only in oocytes of growing follicles.

Concerning the MMP system, macroarray and gelatin zymography revealed that MMP2 is the major collagenase present in the ovary. As already reported (Bagavandoss, 1998), no MMP9 transcripts were detected in neonate rat ovaries. Interestingly, we observed a transient inversion of the ratio between the intermediate inactive and the active forms of MMP2 at the time of follicle assembly. Using in situ zymography in association with laminin immunodetection, we demonstrated that proteasic activity of MMP2 colocalized with the neosynthesized BM within the fragmenting ovigerous cords. Thus, these data point out the close correlation between synthesis and degradation of BM during epithelial restructuration. As MMP2 transcripts are localized in the mesenchymal tissue, it can be predicted that proMMP2 is synthesized by mesenchymal cells and activated by MT1-MMP which is upregulated at the transcript level in epithelial, mesenchymal cells, and oocytes. As described in several tissues, a canonical MMP2/MT1–MMP/TIMP2 complex for MMP2 maturation could be expected (Curry and Osteen, 2001; Ny et al., 2002). TIMP2, however, was detected neither by macroarrays nor by immunofluorescence (data not shown). In contrast, TIMP3, which is an alternative MT1-MMP inhibitor partner (Will et al., 1996), was detected by macroarray. Its antigen was found in the mesenchymal compartment, in agreement with the fact that it is a secreted inhibitor that is associated to the extracellular matrix (Leco et al., 1994). It is well known, however, that MT1-MMP is able to display gelatinolytic activity independently of MMP2 (Curry and Osteen, 2001; Ny et al., 2002). Our results suggest that the different cellular types play complementary roles in the synthesis of the elements of the MMP2/MT1-MMP system in which TIMP3 may be the major tissular regulatory element.

Our in vitro study shows that blockage of follicle histogenesis can be provoked using serine protease inhib-

itors such as aprotinin or leupeptin, which affect enzymes of the plasmin system. Given that mice knocked out for uPA, tPA, both uPA and tPA, or plasminogen display a normal follicle assembly (Ny et al., 2002), it must be hypothesized that aprotinin and leupeptin can indirectly interfere with the MMP system. Indeed, MT1-MMP maturation is achieved by serine proteases: either furin in the golgi apparatus (Sato et al., 1996) or plasmin at the cell surface (Mazzieri et al., 1997; Okumura et al., 1997; Strongin et al., 1995). The final maturation of MMP2, which is generally realized by MT1-MMP, can also be achieved by plasmin (Baramova et al., 1997; Curry and Osteen, 2001; Ny et al., 2002). Moreover, it is possible that the plasmin system maturates proteases that are either unknown or could not be screened by the macroarray, such as cathepsins or members of the ADAM family that play a crucial role during the ovulatory process (Robker et al., 2000).

Epithelial morphogenesis commonly corresponds to two different schemes: mesenchyme-to-epithelium transition or branching morphogenesis (Gumbiner, 1996). In mesenchyme-to-epithelium transition, activated mesenchymal cells aggregate, become surrounded by a continuous BM, and acquire the epithelial phenotype. In branching morphogenesis, preexisting epithelia are submitted to repetitive epithelial cleft and bud formation that are regulated by local synthesis, deposition, and turnover of ECM components, resulting in complex three-dimensional structures. Both processes can be associated in organ morphogenesis, as, for example, in kidney organogenesis (Stuart et al., 1995). Given that follicles arise from preexisting epithelial structures, that is, the ovigerous cords, follicle assembly processes are most likely related to branching morphogenesis. Ovarian morphogenesis exhibits, however, certain specificities. Unlike in branching morphogenesis where intense proliferation of epithelial cells is a prerequisite for bud formation, in ovarian differentiation, epithelial cells are quiescent at the time of follicle histogenesis and proliferate later as follicles leave the resting pool (Hirshfield and DeSanti, 1995). Proliferation of epithelial cells is specific to the process of follicle maturation and not to follicle morphogenesis. Also, in branching morphogenesis, mesenchymal cells that are considered to play an inductive role in morphogenetic processes establish contacts with epithelial cells at the tip of the buds when BM is destroyed (Stuart et al., 1995). In the ovary, the contribution of mesenchymal cells is not obvious. No contacts between pregranulosa and mesenchymal cells at the time of follicle histogenesis were observed. The deposition of the follicular BM precedes the migration of mesenchymal cells in deepening clefts (this study and Merchant-Larios and Chimal-Monroy, 1989). In sheep, follicular units differentiate and become surrounded by a neo-synthesized BM within the ovigerous cords before they cleave (Sawyer et al., 2002). These observations together with the absence of modifications in expression pattern of genes that we studied may well indicate that mesenchymal cells retain a relative immature status during follicle histogenesis. This is consistent with the fact that the characteristic step of mesenchymal cell differentiation occurs later, around 6 dpn, with the commitment of those cells surrounding follicles into the steroidogenic theca pathway (Gelety and Magoffin, 1997).

Another specificity of follicle morphogenesis is the presence of oocyte as a third partner in the interacting cellular types. Paradoxically, although the presence of oocytes dictates follicle histogenesis, considerable oocyte apoptosis takes place at the time of follicle histogenesis (Beaumont and Mandl, 1962; McGee et al., 1998). Our study has stressed the spatiotemporal correlation between oocyte attrition and BM remodeling. TNFα, which is a cytokine synthesized acutely by oocytes and whose receptors are both in granulosa cells and oocytes (Marcinkiewicz et al., 1994), induces in vitro oocyte apoptosis in neonate rat ovaries (Morrison and Marcinkiewicz, 2002). Interestingly, TNFα has been shown to upregulate MT1-MMP expression in the human skin (Han et al., 2001) and MMP2 expression in the forming ovine corpus luteum (Murdoch and McDonnel, 2002). One could, thus, imagine that oocyte apoptosis may well be an initial event inducing epithelial cell differentiation and further determining BM remodeling. Alternatively, given that the degradation of BM components has been correlated with the process of epithelial cell apoptosis in several models (Allard et al., 2000; Lei et al., 1996; Strange et al., 1992), oocyte apoptosis could result from BM instability. Further experiments should address this question.

As already reported in sheep (Sawyer et al., 2002), the wave of oocyte attrition induces a change in the ratio between oocytes and pregranulosa cells. As a consequence, epithelial cells reorganize around surviving oocytes and initiate their progressive polarization. The apical surface of future follicular cells is determined by the contact with the oocyte. Concomitantly, the basal surface is underlined by the deposition of a continuous BM in the clefts deepening in the fragmenting ovigerous cords. A recent study on cleft formation during branching morphogenesis in salivary gland, kidney, and lung organogenesis has stressed the importance of a transient and focal deposition of fibronectin in deepening clefts (Sakai et al., 2003). Following an initial step of cytoskeletal differentiation (Spooner and Wessells, 1972), the deposition of fibronectin induces the loss of cadherins between epithelial cells and, thus, allows conversion of cell–cell adhesion to cell–matrix adhesion (Sakai et al., 2003). In the ovary, differentiation of epithelial cells expressing acutely laminin α1 as well as proteases MT1-MMP and uPA is associated with the deposition of collagen IV, laminin, and fibronectin in deepening clefts that separate forming follicular units before the migration of mesenchymal cells. The emergence of follicular units from regressing ovigerous cords may well be controlled by molecular mechanisms similar to those underlying cleft formation during branching morphogenesis.

In conclusion, our results demonstrate that BM remodeling during follicle histogenesis involves proteinases of the MMP and plasmin families, namely MMP2 and uPA. A decisive event is the differentiation of epithelial cells, which, together with their redistribution around oocytes, display a change in the expression of laminin α1, uPA, MT1-MMP. The activation of epithelial cells, closely dependent on the presence of oocytes, is instrumental in the epithelial remodeling necessary for the emergence of follicles.

Acknowledgments

We greatly thank O. Stettler, L. Muller, E. Etienne, and M.T. Robin for helpful technical advice and assistance, and J.P. Lefaix and H. Coffigny for animal irradiation. We are also grateful to B. Vandenbunder for providing uPA plasmids and Dr. B. Lane for cytokeratin antibody.

This work was supported by Electricité de France and the Ministère de l'Education Nationale et de la Recherche Scientifique et Technique (MENRST, France). S Mazaud is a recipient of a fellowship from Ligue Nationale contre le Cancer, R. Guyot from Organon (Azko Nobel, France), and C.J. Guigon from MENRST.

References

Allard, S., Adin, P., Gouedard, L., di Clemente, N., Josso, N., Orgebin-Crist, M.C., Picard, J.Y., Xavier, F., 2000. Molecular mechanisms of hormone-mediated Mullerian duct regression: involvement of beta-catenin. Development 127, 3349–3360.

Bagavandoss, P., 1998. Differential distribution of gelatinases and tissue inhibitor of metalloproteinase-1 in the rat ovary. J. Endocrinol. 158, 221–228.

Baramova, E.N., Bajou, K., Remacle, A., L'Hoir, C., Krell, H.W., Weidle, U.H., Noel, A., Foidart, J.M., 1997. Involvement of PA/plasmin system in the processing of pro-MMP-9 and in the second step of pro-MMP-2 activation. FEBS Lett. 405, 157–162.

Beaumont, H.M., Mandl, A.M., 1962. A quantitative and cytological study of oogonia and oocytes in the fetal and neonatal rat. Proc. R. Soc. B 155, 557–579.

Curry Jr., T.E., Osteen, K.G., 2001. Cyclic changes in the matrix metalloproteinase system in the ovary and uterus. Biol. Reprod. 64, 1285–1296.

Duchossoy, Y., Horvat, J.C., Stettler, O., 2001. MMP-related gelatinase activity is strongly induced in scar tissue of injured adult spinal cord and forms pathways for ingrowing neurites. Mol. Cell. Neurosci. 17, 945–956.

Falk, M., Ferletta, M., Forsberg, E., Ekblom, P., 1999. Restricted distribution of laminin alpha1 chain in normal adult mouse tissues. Matrix Biol. 18, 557–568.

Frojdman, K., Ekblom, P., Sorokin, L., Yagi, A., Pelliniemi, L.J., 1995. Differential distribution of laminin chains in the development and sex differentiation of mouse internal genitalia. Int. J. Dev. Biol. 39, 335–344.

Frojdman, K., Pelliniemi, L.J., Virtanen, I., 1998. Differential distribution of type IV collagen chains in the developing rat testis and ovary. Differentiation 63, 125–130.

Frojdman, K., Pelliniemi, L.J., Rey, R., Virtanen, I., 1999. Presence of anti-Mullerian hormone correlates with absence of laminin alpha5 chain in differentiating rat testis and ovary. Histochem. Cell Biol. 111, 367–373.

Gelety, T.J., Magoffin, D.A., 1997. Ontogeny of steroidogenic enzyme gene expression in ovarian theca-interstitial cells in the rat: regulation by a paracrine theca-differentiating factor prior to achieving luteinizing hormone responsiveness. Biol. Reprod. 56, 938–945.

Gu, W., Tekur, S., Reinbold, R., Eppig, J.J., Choi, Y.C., Zheng, J.Z., Murray, M.T., Hecht, N.B., 1998. Mammalian male and female germ cells express a germ cell-specific Y-Box protein, MSY2. Biol. Reprod. 59, 1266–1274.

Gumbiner, B.M., 1996. Cell adhesion: the molecular basis of tissue architecture and morphogenesis. Cell 84, 345–357.

Guyot, R., Magre, S., Leduque, P., Le Magueresse-Battistoni, B., 2003. Differential expression of tissue inhibitor of metalloproteinases type 1 (TIMP-1) during mouse gonad development. Dev. Dyn. 227, 357–366.

Hagglund, A.C., Ny, A., Liu, K., Ny, T., 1996. Coordinated and cell-specific induction of both physiological plasminogen activators creates functionally redundant mechanisms for plasmin formation during ovulation. Endocrinology 137, 5671–5677.

Han, Y.P., Tuan, T.L., Wu, H., Hughes, M., Garner, W.L., 2001. TNF-alpha stimulates activation of pro-MMP2 in human skin through NF-(kappa)B mediated induction of MT1-MMP. J. Cell Sci. 114, 131–139.

Hirshfield, A.N., DeSanti, A.M., 1995. Patterns of ovarian cell proliferation in rats during the embryonic period and the first three weeks postpartum. Biol. Reprod. 53, 1208–1221.

Leco, K.J., Khokha, R., Pavloff, N., Hawkes, S.P., Edwards, D.R., 1994. Tissue inhibitor of metalloproteinases-3 (TIMP-3) is an extracellular matrix-associated protein with a distinctive pattern of expression in mouse cells and tissues. J. Biol. Chem. 269, 9352–9360.

Lei, H., Furth, E.E., Kalluri, R., Chiou, T., Tilly, K.I., Tilly, J.L., Elkon, K.B., Jeffrey, J.J., Strauss III, J.F., 1996. A program of cell death and extracellular matrix degradation is activated in the amnion before the onset of labor. J. Clin. Invest. 98, 1971–1978.

Li, M., Karakji, E.G., Xing, R., Fryer, J.N., Carnegie, J.A., Rabbani, S.A., Tsang, B.K., 1997. Expression of urokinase-type plasminogen activator and its receptor during ovarian follicular development. Endocrinology 138, 2790–2799.

Longin, J., Guillaumot, P., Chauvin, M.A., Morera, A.M., Le Magueresse-Battistoni, B., 2001. MT1-MMP in rat testicular development and the control of Sertoli cell proMMP-2 activation. J. Cell Sci. 114, 2125–2134.

Marcinkiewicz, J.L., Krishna, A., Cheung, C.M., Terranova, P.F., 1994. Oocytic tumor necrosis factor alpha: localization in the neonatal ovary and throughout follicular development in the adult rat. Biol. Reprod. 50, 1251–1260.

Mazaud, S., Guigon, C.J., Lozach, A., Coudouel, N., Forest, M.G., Coffigny, H., Magre, S., 2002. Establishment of the reproductive function and transient fertility of female rats lacking primordial follicle stock after fetal gamma-irradiation. Endocrinology 143, 4775–4787.

Mazzieri, R., Masiero, L., Zanetta, L., Monea, S., Onisto, M., Garbisa, S., Mignatti, P., 1997. Control of type IV collagenase activity by components of the urokinase–plasmin system: a regulatory mechanism with cell-bound reactants. EMBO J. 16, 2319–2332.

McGee, E.A., Hsu, S.Y., Kaipia, A., Hsueh, A.J., 1998. Cell death and survival during ovarian follicle development. Mol. Cell. Endocrinol. 140, 15–18.

McLaren, A., 1991. Development of the mammalian gonad: the fate of the supporting cell lineage. Bioessays 13, 151–156.

Merchant-Larios, H., Chimal-Monroy, J., 1989. The ontogeny of primordial follicles in the mouse ovary. Prog. Clin. Biol. Res. 296, 55–63.

Morrison, L.J., Marcinkiewicz, J.L., 2002. Tumor necrosis factor alpha enhances oocyte/follicle apoptosis in the neonatal rat ovary. Biol. Reprod. 66, 450–457.

Murdoch, W.J., McDonnel, A.C., 2002. Roles of the ovarian surface epithelium in ovulation and carcinogenesis. Reproduction 123, 743–750.

Ny, T., Wahlberg, P., Brandstrom, I.J., 2002. Matrix remodeling in the

ovary: regulation and functional role of the plasminogen activator and matrix metalloproteinase systems. Mol. Cell. Endocrinol. 187, 29–38.

Odet, F., Guyot, R., Leduque, P., Le Magueresse-Battistoni, B., 2004. Evidence for similar expression of protein C inhibitor and the urokinase-type plasminogen activator system during mouse testis development. Endocrinology 145, 1481–1489.

Okumura, Y., Sato, H., Seiki, M., Kido, H., 1997. Proteolytic activation of the precursor of membrane type 1 matrix metalloproteinase by human plasmin. A possible cell surface activator. FEBS Lett. 402, 181–184.

Pelliniemi, L.J., Frojdman, K., 2001. Structural and regulatory macromolecules in sex differentiation of gonads. J. Exp. Zool. 290, 523–528.

Pepling, M.E., Spradling, A.C., 2001. Mouse ovarian germ cell cysts undergo programmed breakdown to form primordial follicles. Dev. Biol. 234, 339–351.

Rajah, R., Sundaram, G.S., 1994. Protein distribution and gene expression of collagen type IV in the neonatal rat ovary during follicle formation. Cell. Mol. Biol. (Noisy-le-grand) 40, 769–780.

Rajah, R., Glaser, E.M., Hirshfield, A.N., 1992. The changing architecture of the neonatal rat ovary during histogenesis. Dev. Dyn. 194, 177–192.

Robker, R.L., Russell, D.L., Yoshioka, S., Sharma, S.C., Lydon, J.P., O'Malley, B.W., Espey, L.L., Richards, J.S., 2000. Ovulation: a multigene, multi-step process. Steroids 65, 559–570.

Rodgers, R.J., Irving-Rodgers, H.F., van Wezel, I.L., 2000. Extracellular matrix in ovarian follicles. Mol. Cell. Endocrinol. 163, 73–79.

Sakai, T., Larsen, M., Yamada, K.M., 2003. Fibronectin requirement in branching morphogenesis. Nature 423, 876–881.

Sato, H., Kinoshita, T., Takino, T., Nakayama, K., Seiki, M., 1996. Activation of a recombinant membrane type 1-matrix metalloproteinase (MT1-MMP) by furin and its interaction with tissue inhibitor of metalloproteinases (TIMP)-2. FEBS Lett. 393, 101–104.

Sawyer, H.R., Smith, P., Heath, D.A., Juengel, J.L., Wakefield, S.J., McNatty, K.P., 2002. Formation of ovarian follicles during fetal development in sheep. Biol. Reprod. 66, 1134–1150.

Spooner, B.S., Wessells, N.K., 1972. An analysis of salivary gland morphogenesis: role of cytoplasmic microfilaments and microtubules. Dev. Biol. 27, 38–54.

Strange, R., Li, F., Saurer, S., Burkhardt, A., Friis, R.R., 1992. Apoptotic cell death and tissue remodelling during mouse mammary gland involution. Development 115, 49–58.

Strongin, A.Y., Collier, I., Bannikov, G., Marmer, B.L., Grant, G.A., Goldberg, G.I., 1995. Mechanism of cell surface activation of 72-kDa type IV collagenase. Isolation of the activated form of the membrane metalloprotease. J. Biol. Chem. 270, 5331–5338.

Stuart, R.O., Barros, E.J., Ribeiro, E., Nigam, S.K., 1995. Epithelial tubulogenesis through branching morphogenesis: relevance to collecting system development. J. Am. Soc. Nephrol. 6, 1151–1159.

Tolli, R., Monaco, L., Di Bonito, P., Canipari, R., 1995. Hormonal regulation of urokinase- and tissue-type plasminogen activator in rat Sertoli cells. Biol. Reprod. 53, 193–200.

Vu, T.H., Werb, Z., 2000. Matrix metalloproteinases: effectors of development and normal physiology. Genes Dev. 14, 2123–2233.

Will, H., Atkinson, S.J., Butler, G.S., Smith, B., Murphy, G., 1996. The soluble catalytic domain of membrane type 1 matrix metalloproteinase cleaves the propeptide of progelatinase A and initiates autoproteolytic activation. Regulation by TIMP-2 and TIMP-3. J. Biol. Chem. 271, 17119–17123.